AFRL-RB-WP-TP-2012-0162

HIGH-TEMPERATURE LIQUID METAL TRANSPORT PHYSICS OF CAPILLARY PUMPING HEAT TRANSPORT SYSTEM (CPHTS) RESEARCH

Experimental and Theoretical Studies of Evaporating Liquid Metal Thin Film

Ryan E. Mikus

Advanced Structural Concepts Branch
Structures Division

Kenneth D. Kihm

University of Tennessee

APRIL 2012
Interim

Approved for public release; distribution unlimited.

See additional restrictions described on inside pages

STINFO COPY

AIR FORCE RESEARCH LABORATORY
AIR VEHICLES DIRECTORATE
WRIGHT-PATTERSON AIR FORCE BASE, OH 45433-7542
AIR FORCE MATERIEL COMMAND
UNITED STATES AIR FORCE

REPORT DOCUMENTATION PAGE

Form Approved OMB No. 0704-0188

1. REPORT DATE *(DD-MM-YY)*	2. REPORT TYPE	3. DATES COVERED *(From - To)*
April 2012	Interim	01 February 2011 – 12 April 2012

4. TITLE AND SUBTITLE

HIGH-TEMPERATURE LIQUID METAL TRANSPORT PHYSICS OF CAPILLARY PUMPING HEAT TRANSPORT SYSTEM (CPHTS) RESEARCH

Experimental and Theoretical Studies of Evaporating Liquid Metal Thin Film

5a. CONTRACT NUMBER
In-house

5b. GRANT NUMBER

5c. PROGRAM ELEMENT NUMBER
61102F

6. AUTHOR(S)

Ryan E. Mikus (AFRL/RBSA)
Kenneth D. Kihm (University of Tennessee)

5d. PROJECT NUMBER
2303

5e. TASK NUMBER

5f. WORK UNIT NUMBER
A03I0D

7. PERFORMING ORGANIZATION NAME(S) AND ADDRESS(ES)

Advanced Structural Concepts Branch (AFRL/RBSA)
Structures Division
Air Force Research Laboratory, Air Vehicles Directorate
Wright-Patterson Air Force Base, OH 45433-7542
Air Force Materiel Command, United States Air Force

University of Tennessee

8. PERFORMING ORGANIZATION REPORT NUMBER
AFRL-RB-WP-TP-2012-0162

9. SPONSORING/MONITORING AGENCY NAME(S) AND ADDRESS(ES)

Air Force Research Laboratory
Air Vehicles Directorate
Wright-Patterson Air Force Base, OH 45433-7542
Air Force Materiel Command
United States Air Force

10. SPONSORING/MONITORING AGENCY ACRONYM(S)
AFRL/RBSA

11. SPONSORING/MONITORING AGENCY REPORT NUMBER(S)
AFRL-RB-WP-TP-2012-0162

12. DISTRIBUTION/AVAILABILITY STATEMENT
Approved for public release; distribution unlimited.

13. SUPPLEMENTARY NOTES
PAO Case Number: 88ABW-2012-2876; Clearance Date: 16 May 2012. Paper contains color.

14. ABSTRACT

The objective of this research is to experimentally and theoretically study multi-scale heat and mass transport phenomena in evaporating liquid sodium thin film using a specially designed test vessel at the Facility for Innovative Research in Structures Technology (FIRST) Laboratory in Building 65 at Wright-Patterson Air Force Base (WPAFB).

15. SUBJECT TERMS
thin film sodium, heat and mass transport physics, liquid metal sodium, evaporating sodium

16. SECURITY CLASSIFICATION OF: a. REPORT	b. ABSTRACT	c. THIS PAGE	17. LIMITATION OF ABSTRACT:	18. NUMBER OF PAGES	19a. NAME OF RESPONSIBLE PERSON (Monitor)
Unclassified	Unclassified	Unclassified	SAR	14	Ryan E. Mikus
					19b. TELEPHONE NUMBER *(Include Area Code)* N/A

■ RESEARCH OBJECTIVE

The objective of this research is to experimentally and theoretically study multi-scale heat and mass transport phenomena in evaporating liquid sodium thin film using a specially designed rig at the Facility for Innovative Research in Structures Technology (FIRST) Laboratory in Building 65 at Wright-Patterson Air Force Base (WPAFB).

■ PROPOSED TASKS

I. Experimental characterization of evaporating liquid sodium (Na) thin film inside a high-temperature working heat pipe using the neutron imaging facility available through National Institute of Standards and Technology (NIST).

II. Theoretical predictions and parametric studies of multi-scale heat and mass transport physics of evaporative thin film and bulk meniscus of liquid Na coolant.

■ SUMMARY OF ACHIEVEMENT

1. Experimental Characterization of Sodium Capillary Inside a Heat Pipe

The primary achievement of the task was to make it possible to non-intrusively characterize the liquid metal Sodium (Na) behavior inside a heat pipe using a neutron imaging technique. Preliminary results using the neutron imager at National Institute of Standards and Technology (NIST) showed good feasibility of neutron imaging of liquid Sodium contained inside an alloy jacket.

Neutron wave imaging has an inherent advantage compared with the x-ray imaging because it requires relatively low energy intensity to penetrate metals: Fig. 1-A shows that the neutron wave scattering cross sections decrease to a greater or lesser extent with increasing material densities. Thus, neutron radiography allows highly effective visualization of the dynamics of the fluid in the metal environment while there are minimal to no changes in the thermal properties of the overall system [1-3]. For example, the water contained in Asiatic lilies provides the fine details for its neutron image even in a lead cask (Fig. 1-B).

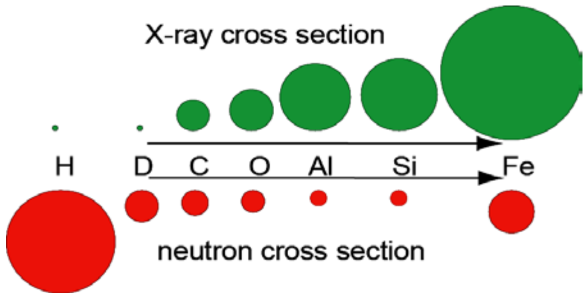

(A)

(B)

Figure 1 (A) Neutron cross-sectional areas of different atoms, compared with x-ray cross sections, and (B) highly detailed neutron image of Asiatic lilies in a lead cask because of the extremely large cross-section of hydrogen atoms.

Most neutron imaging facilities are located at fission reactors, and make use of a thermal neutron energy spectrum, which can be described by a Maxwell-Boltzmann energy distribution. At the NIST neutron imaging facility (Fig. 2), there are a range of collimation ratios and fluency rates available, to optimize the beam conditions for the sample under study.

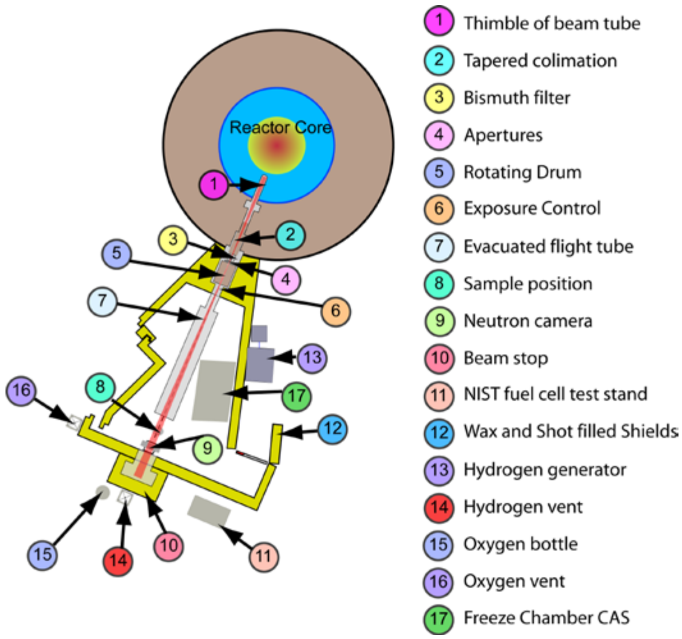

Figure 2 Schematic layout of the neutron imaging facility at National Institute of Standards and Technology (NIST) in Gaithersburg, Maryland.

Preliminary testing has been performed with a nickel alloy heat pipe (Thermacore Inc., Lancaster, PA) of 3-mm x 10-mm rectangular cross-section, 150-mm length, under ambient temperature condition. Thus, the contrast shown in the transmission images (Fig. 3) indicates solidified sodium that is exposed to neutron beam for 100s. Table 1 presents the basic properties of liquid sodium, and Table 2 summarizes the thermo-electric properties of different materials. Calculations using the Lambert-Beer beam attenuation governing equations shows that the 3-mm thick sodium slab provides only 3% contrast differential with the background intensity of sodium-free zones. Further studies are planned to carefully examine the imaging capabilities toward enhancing both spatial and temporal imaging resolutions.

Fundamental findings that are available from this preliminary imaging study include:

- Neutron radiography has detectable contrast for sodium, and can easily penetrate the metal heat pipe walls.
- The contrast is low, about a 3% change in transmission for the 3 mm sodium slug.
- The low contrast for sodium will require tradeoffs in field of view; temporal resolution; and spatial resolution.
- The present composition of the metal housing doesn't limit the measurement uncertainty.

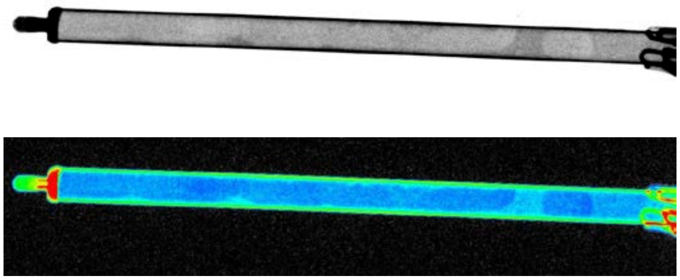

(A)

(B)

Figure 3 (A) Neutron transmission image of solidified sodium inside a nickel-alloy heat pipe, and (B) corresponding false-color image. The image dimension is 10-mm high and 150-mm long and the exposure time of 100 seconds.

TABLE 1

Property	Liquid Sodium (Na)	Water (H2O)
Evaporation Temperature	1156.1 K	373.15 K
Melting Temperature	371 K	273.15 K
Specific Gravity	0.927 (l)	1.0
Dynamic Viscosity	1.5839E-4 N-s/m2	1.002E-3 N-s/m2
Surface Tension	0.1197 N/m	0.0728 N/m
Thermal Conductivity (300K)	142 W/m-K	0.5984 W/m-K
Latent Heat of Vaporization	3879.5 KJ/kg	2441.2 KJ/kg
Electric Conductivity	2.5361E+6 S/m	5.5E-6 S/m
Magnetic Ordering	Paramagnetic	Nonmagnetic

TABLE 2

Substances	Thermal Conductivity [W/m·K]	Electrical Resistivity [nΩ·m]	Boiling/Melting Temperatures [K]
Water	0.58	18.2 x 10E+13	373/273
Copper	400	16.78	2835/1358
Sodium	142	47.7	1156/371
Molybdenum	138	53.4	4912/2896
Niobium	53.7	152	5017/2750
Quartz	1.4	7 x 10E+14	NA/1670
Glass	1.005 (Pyrex)	10E+23 at 20C 10E+12 at 1500C	NA/1000
Sapphire	41.9	10E+23 at 20C 10E+18 at 1500C	NA/2313

2. Multi-Scale Theoretical Characterization of Evaporating Sodium Capillary

A new multi-scale model [4] allows predicting the heat and mass transport behaviors of the evaporating liquid metal capillary meniscus under evaporation, as schematically shown in Fig. 4. Among the three distinct regions, the adsorption film does not contribute to evaporation since the ultra thin layer of liquid molecules is strongly held by the metal surface molecules under van-der-Waals interactions. The model scope is then two-fold: (1) the micro/nano-scale modeling of the transition thin film region, and (2) the macro-scale CFD modeling of the intrinsic or bulk meniscus region.

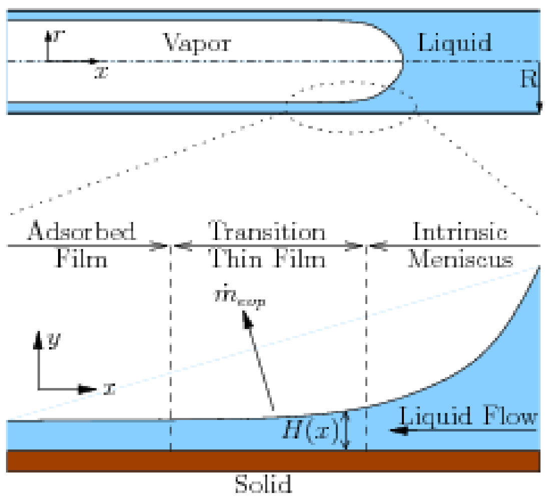

Figure 4 Schematic of liquid capillary geometry identifying the distinct three regions of the multi-scale evaporating meniscus: (1) the atomic-scale adsorbed film region, (2) micro-nanoscale transition thin film region, and (3) the macro-scale intrinsic (or bulk) meniscus region.

The key of the transition thin film modeling is the disjoining pressure that determines the formation of thin liquid film and then the evaporative mass flux along the interface. For nonmetallic coolants, the disjoining pressure term is solely represented by the London-van der Waals dispersion (Π_A). For the case of metallic coolants, however, the abundant free electrons must additionally contribute to the disjoining pressure since they will experience a confinement when the liquid metal is squeezed into a thin film. Consequently, this electron degeneracy can create an increase of the energy density and produces an additional “electronic disjoining pressure” (Π_B).

The intrinsic meniscus CFD modeling uses COMSOL Multi-physics Finite Element software package to simultaneously solve the appropriate mass, momentum and energy equations. The solutions for the intrinsic meniscus will be integrated with the solutions from the transition thin film model to create a comprehensive multi-scale model of evaporating liquid metal capillary.

Comparative studies have been conducted to examine the exclusive effect of the additional disjoining pressure by free electrons on the thin film profiles as well as on the evaporative mass flux under identical heating conditions. It is shown that the existence of electronic component of the disjoining pressure leads towards larger total capillary meniscus surface area (Figs. 5A and B), and therefore, larger net evaporative mass flow rate (Fig. 5C). Note that the bold lines show the calculation results with properly accounting for the electronic disjoining pressure for sodium ($\Pi_B/\Pi_A = 98.68$) and the regular lines represent the solutions with neglecting any contributions from the free electrons ($\Pi_B/\Pi_A = 0$).

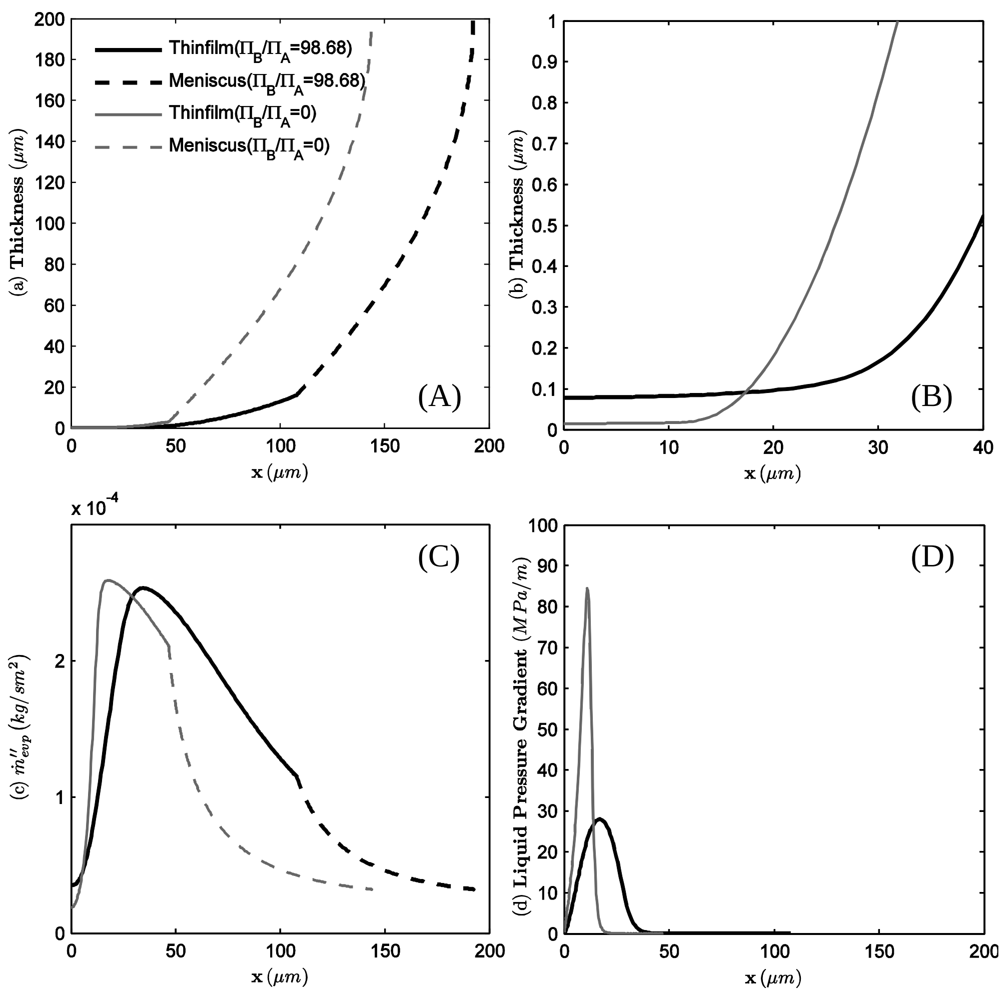

Figure 5 Theoretical predictions of evaporating sodium capillary meniscus behaviors: (A) sodium thickness profiles for 0 < x < 200 μm, spanning both the transition thin film region and the matching intrinsic (bulk) meniscus region, (B) enlarged thin film thickness profiles for 0 < x < 40 μm, (C) evaporative mass flux distributions, and (D) Disjoining pressure gradient inside the sodium liquid.

Furthermore, it is found that the net evaporative mass flux in the bulk meniscus region must be accounted for to obtain a true picture of the total capillary evaporation transport for liquid sodium. For the case of a moderate coolant such as water, the evaporative flux from the intrinsic meniscus is usually negligible since the excessively high thermal resistance associated with the bulk thickness limits the liquid-vapor interface temperature below the evaporation onset. This is not the case for the case of liquid metal coolants such as sodium as the thermal conductivity of metal is about two orders of magnitude higher than that of ordinary coolants containing no free electrons (see Table 1 or Table 2).

The important conceptual findings identified from the present work include the following:

1. Accurate high temperature, liquid metal, capillary evaporation models for liquid metal coolants should account for both the London-van der Waals dispersion (Π_A) and the electronic disjoining pressures (Π_B) in the extended thin film regime.
2. Unlike more traditional or non-metallic coolants, evaporative mass and heat flow occurs in the intrinsic bulk meniscus region of evaporating micro-capillaries.
3. The clear trend from these comparisons is that a larger electronic component of the disjoining pressure leads towards larger extended meniscus thin film surface area, larger total capillary meniscus surface area, and larger net evaporative mass flow rate.

■ FUTURE DIRECTIONS

1. Neutron radiography experiment will be extended to characterize the evaporating capillary meniscus of lithium coolant that has substantially larger cross-section to result in more distinctive shadows than sodium.

2. Theoretical characterization using the electronic degeneracy concept will be extended to predict evaporating lithium capillary transport behaviors and the results will be compared with those of evaporating liquid sodium meniscus.

3. In order to physically elaborate both experimental and theoretical characterization results of liquid metals, knowledge on the surface energy or surface tension coefficients is necessary but unavailable for different substrate types (molybdenum, niobium, their alloys etc.) and morphology (surface roughness, wicking shape and dimensions etc.) in need for heat pipe designs. Therefore, a new experiment will be devised using a goniometer to measure the wetting angles and surface energy levels of liquid metal drops for carefully selected substrate samples at different temperatures.

References

[1] T. A. Trabold, J. P. Owejan, J. J. Gagliardo, D. L. Jacobson, D. S. Hussey and M. Arif, "Use of neutron imaging for proton exchange membrane fuel cell (PEMFC) performance analysis and design", Handbook of Fuel Cells - Fundamentals, Technology and Applications, Volume 6. Edited by Wolf Vielstich, Harumi Yokokawa, Hubert A. Gasteiger. 2009 John Wiley & Sons, Ltd.

[2] N.Takenaka, K.Sugimoto, H.Kawami, T.Yoshida, “Visualization of Two-Phase Flow Phenomena in A Self-Vibration Heat Pipe By Neutron Radiography”, *The Eighteenth International Symposium on Transport Phenomena*, 27-30 August, 2007, Daejeon, *KOREA.*

[3] B. Borgmeyer, C. Wilson, R. A. Winholtz, H. B. Ma, D. Jacobson, D. Hussey, 2010, “Heat Transport Capability and Fluid Flow Neutron Radiography of Three-Dimensional Oscillating Heat Pipes”, Journal of Heat Transfer, 132.

[4] Tipton Jr, J. B., Kihm, K. D., and Pratt, D. M., 2009, "Modeling Alkaline Liquid Metal (Na) Evaporating Thin Films Using Both Retarded Dispersion and Electronic Force Components," Journal of Heat Transfer, 131, 121015-9.